Carbohydrate Research 345 (2010) 1461–1468

Contents lists available at ScienceDirect

Carbohydrate Research

journal homepage: www.elsevier.com/locate/carres

Effect of a serine-to-aspartate replacement on the recognition of chitin oligosaccharides by truncated hevein. A 3D view by using NMR

María Isabel Chávez [a,c,†], Miquel Vila-Perelló [b,†], Francisco Javier Cañada [a,*], David Andreu [b,*], Jesús Jiménez-Barbero [a,*]

[a] Chemical and Physical Biology, Centro de Investigaciones Biológicas, CSIC, Ramiro de Maeztu 9, 28040 Madrid, Spain
[b] Departament de Ciències Experimentals i de la Salut, Universitat Pompeu Fabra, Dr. Aiguader 88, 08003 Barcelona, Spain
[c] Instituto de Química, Universidad Nacional Autónoma de México, 04510, Coyoacán, Circuito Exterior, México D.F., Mexico

ARTICLE INFO

Article history:
Received 23 December 2009
Received in revised form 11 February 2010
Accepted 20 February 2010
Available online 25 February 2010

Keywords:
Molecular recognition
Carbohydrates
Three-dimensional structure
NMR
Lectins

ABSTRACT

The interaction of a synthetically prepared mutant peptide of hevein (a well known chitin-binding lectin) Hev32S19D with chitin oligosaccharides (and chitosan analogues) has allowed us to estimate their affinity constants and associated thermodynamic data. The mutant peptide is able to bind chitin oligomers, but with significant decreases in the association constants with chito-oligosaccharides. The determination of the three-dimensional structure of the peptide mutant, by using NMR, has permitted us to deduce that the topology of the backbone is very similar to that of the parent Hev32 peptide. The same is true regarding the orientations of the key aromatic residues Trp21, Trp23, and Tyr30. The decrease in the association constants can be attributed to the different topological orientation of key side chains and to the importance of protein–sugar intermolecular essential hydrogen bonds and CH–π stacking interactions. The analysis has permitted us to infer the free energy of binding associated with these interactions as well as to estimate the corresponding binding enthalpy.

© 2010 Elsevier Ltd. All rights reserved.

1. Introduction

In recent years, research on glycosciences has been greatly encouraged due to the unequivocal demonstration of the pivotal role of carbohydrates in a variety of physiological processes from immune and inflammatory responses, organogenesis, metastasis, to diverse infectious processes.[1–3]

X-ray crystallography and NMR spectroscopy have been used to determine the three-dimensional structures of diverse hevein domains (Scheme 1),[2–5] both in the free and in the carbohydrate-associated state. Analysis of the structures has shown that van der Waals and stacking interactions together with hydrogen bonds play a crucial role in the modulation of the selectivity and stability of the protein–carbohydrate complex.[6–15] Thus, hevein domains have been used as simple interaction models to better understand the key elements involved in protein–chito-oligosaccharide interactions. We have recently shown that a truncated hevein domain encompassing its 32N-terminal amino acids only lost 20% of the affinity in relation to native hevein, towards *N′*,*N″*,*N‴*-triacetylchitotriose $(GlcNAc)_3$.[17] The previous studies mentioned above have allowed corroborating that many non-polar contacts involve one of the faces of the sugar ring interacting with the aromatic rings of Trp, Phe and Tyr side chains.[16]

For hevein, the key aromatic amino acids Trp21 and Trp23 stabilize the complexes by means of stacking CH–π interactions. Also, van der Waals interactions take place between Tyr30 and the methyl group of the acetamide moiety of the sugar. Every CH–π stacking interaction was demonstrated to add ~1.8 kcal/mol to the stabilization of the complex. In addition, the hydroxyl groups of Tyr30 and Ser19 intervene through hydrogen bonds with OH-3 of the sugar residue and with the carbonyl group of the acetamide moiety, respectively, but the energetic contribution of such interactions has not yet been evaluated.

On the basis of the structural information described above, and as part of our ongoing studies to elucidate the relative importance of the different interactions involved in protein–carbohydrate recognition, we sought to quantify the energy value for the key hydrogen bond interaction between Ser19 and the carbonyl moiety of the carbohydrate. The mutation of the key Ser19 residue to another polar amino acid of the same side-chain length but without an H-bond donor group should allow us to perform such measurements. Thus, an analogue of the truncated hevein domain (Hev32)[17] was synthesized where Ser19 was mutated to Asp (Hev32S19D). This mutation could, in turn, provide a peptide able to recognize a chitosan fragment $GlcNH_2(GlcNAc)_4$, which lacks one of the *N*-acetamide moieties at the non-reducing end (Scheme 1), by forming a salt bridge between the NH_3, at the non-reducing end

* Corresponding authors.
E-mail address: jjbarbero@cib.csic.es (J. Jiménez-Barbero).
† These two authors have equally contributed to this work.

0008-6215/$ - see front matter © 2010 Elsevier Ltd. All rights reserved.
doi:10.1016/j.carres.2010.02.019

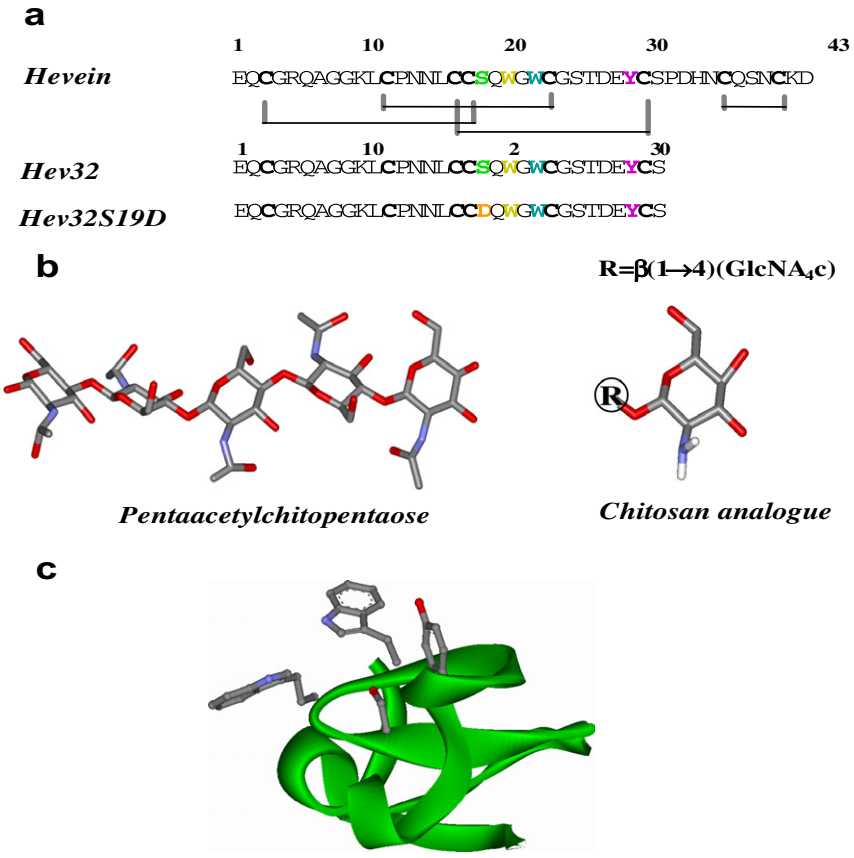

Scheme 1. (a) Amino acid sequence of hevein (indicating the disulfide bridge pattern), truncated hevein (Hev32) and the designed mutant peptide (Hev32S19D). (b) Chemical structures of N,N',N'',N''',N''''-penta-acetylchitopentaose and its N,N',N'',N'''-tetraacetyl derivative (chitosan-like derivative). The key amino acids in the primary sequences are highlighted. (c) Schematic view of the folding of hevein, showing the orientation of the key amino acids for GlcNAc binding.

glucosamine (pK around 6.7),[18] and the carboxylate of Asp19, with a pK around 4.8[19] (shown in Scheme 2). Moreover, because the chosen chitosan fragment lacks the non-reducing end acetamide group, which interacts with the aromatic ring of Tyr30, the strength of the van der Waals interaction between Tyr30 and the acetamide methyl moiety could also be estimated (Schemes 1 and 2).

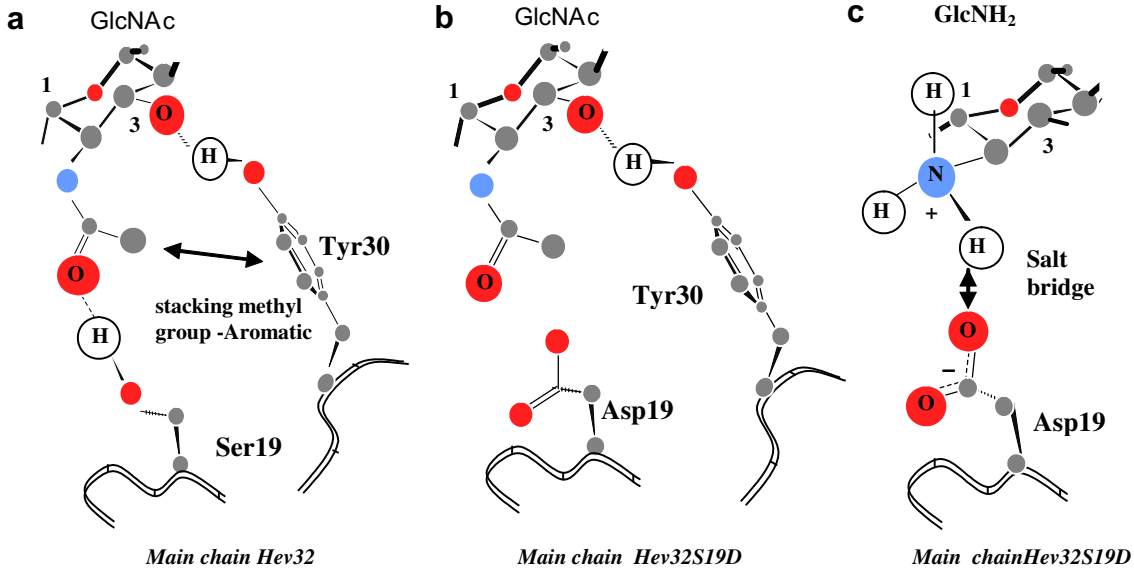

Scheme 2. (a) Schematic representation of hydrogen bonds between the OH group of Ser19 with the acetamide carbonyl and of the OH of Tyr30 with GlcNAc OH-3. (b) As hypothesized, the S19D mutation could preclude the proper establishment of the Ser19 hydrogen bond, and the possibly disturbs the stacking interaction between the acetamide moiety and the Tyr aromatic ring. (c) A hypothetical interaction between the carboxyl group of D19 and the non-reducing end of a chitosan-like derivative $GlcNH_2(GlcNAc)_4$ could take place. The employment of a longer amino acid side chain, with glutamic acid, could introduce additional entropic costs, due to the additional torsional degrees of freedom.

2. Results and discussion

2.1. Ligand-binding studies

The association between the mutant peptide Hev32S19D and $(GlcNAc)_5$ or $GlcNH_2(GlcNAc)_4$ was studied by 1D ^1H NMR titrations following the procedure described in the materials and methods section, which is based on the analysis of 1D spectra recorded for series of samples containing a constant concentration of polypeptide with increasing ligand concentrations.[17]

Spectra were obtained at four different temperatures (Fig. 1), and the observed perturbations in the chemical shifts of the peptide upon sugar addition clearly proved the formation of specific complexes between Hev32S19D and different chitin ($(GlcNAc)_{3-5}$) and chitosan $GlcNH_2(GlcNAc)_4$) derivatives. A slight broadening of the NMR signals of the peptide upon addition of either carbohydrate was observed, thus indicating that the processes of exchange between the free and bound states are fast enough in the chemical shift NMR time scale to use titration curves to estimate the binding affinities. The association constants (K_a) were thus determined by non-linear least-square fitting of the observed chemical shifts perturbations versus different ligand–receptor molar ratios. Different protons are available for the titration analysis, and their variations plotted as a function of the concentration of the added carbohydrate to determine the binding constant values (Fig. 2a and b). The representation of the variation of K_a values versus the inverse of the temperature allowed qualitatively estimating the thermodynamic parameters ΔH° and ΔS° (Table 1), from the van't Hoff plot (Fig. 3).

The association constant (K_a) and the thermodynamic parameters (Table 1) obtained for the Hev32S19D–$(GlcNAc)_3$ complex allowed us to conclude that the mutant peptide is still able to bind *N*-acetylglucosamine derivatives, but with moderate affinity. Indeed, the experimental K_a value for the Hev32S19D–$(GlcNAc)_3$ interaction is almost half of that described for Hev32 with the same chitin trisaccharide and more than two orders of magnitude smaller than that determined for the interaction of full length hevein with the pentasaccharide, using microcalorimetry (ITC).[20] In this case, the large K_a precluded its determination by NMR, while analytical ultracentrifugation and NMR-DOSY studies permitted us to demonstrate that the high affinity value for the hevein_$(GlcNAc)_5$ complex was partially due to the existence of high stoichiometry complexes (above 1:1), where more than one hevein domain could be attached to one oligosaccharide chain.

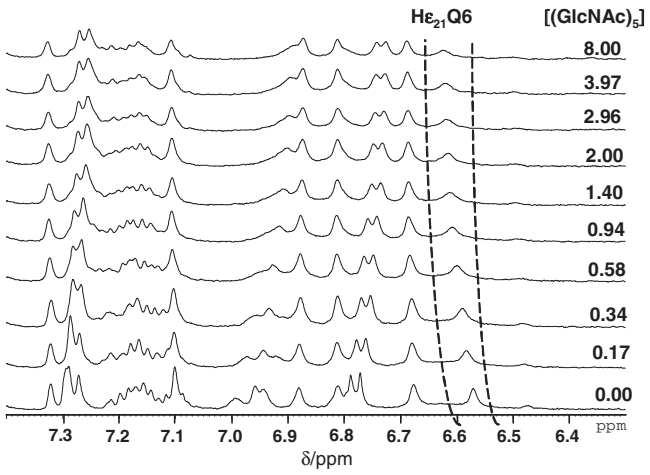

Figure 1. NMR titration of Hev32S19D (0.28 mM) with increasing amounts (mM concentrations are given at the right hand side) of $(GlcNAc)_3$ at 303 K and pH 5.6. The variation of the $H\varepsilon_{21}$ of Q6 can be easily followed.

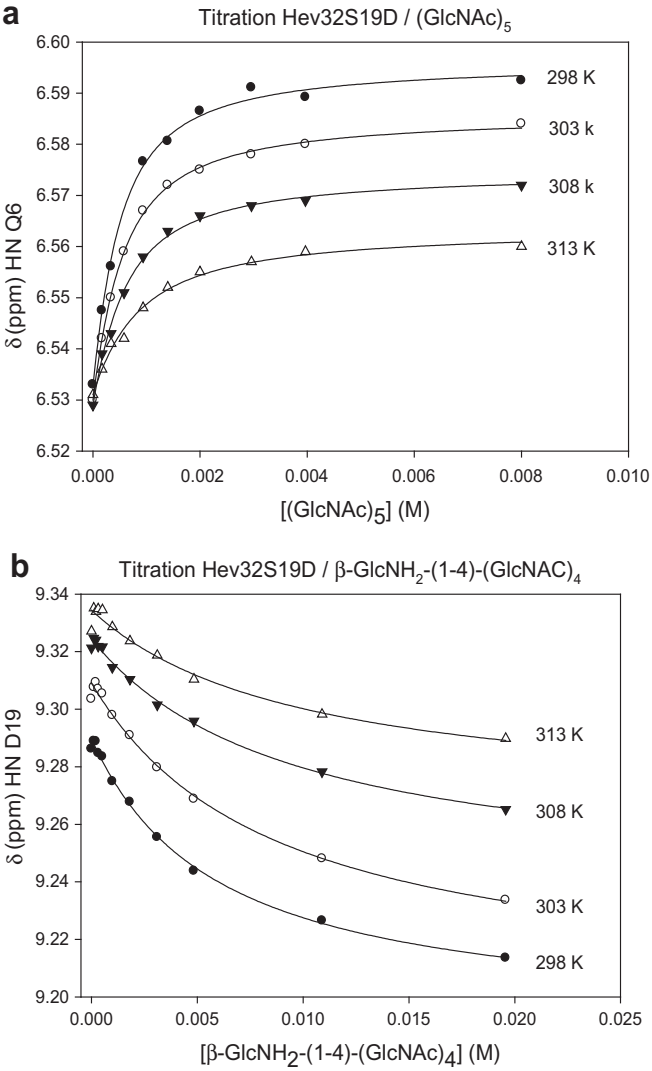

Figure 2. Analysis of the interaction of $(GlcNAc)_5$ and $GlcNH_2(GlcNAc)_4$ binding to Hev32S19D determined by NMR. (a) Binding curves derived from NMR titration for association of $(GlcNAc)_5$ to Hev32S19D. (b) Binding curves derived from NMR titration for association of $GlcNH_2(GlcNAc)_4$ to Hev32S19D. (c) van't Hoff plot of ln K_a versus $1/T$ for both complexes

Nonetheless, in the present study, for the binding of the chito-oligosaccharides $(GlcNAc)_3$ and $(GlcNAc)_5$ to Hev32S19D, a good fit was obtained for a 1:1 model (Table 1).[17,21] The thermodynamic parameters, ΔH° and ΔS°, were obtained from a van't Hoff plot of $\ln(K_a)$ versus $1/T$. It should be recognized that the use of van't Hoff plots should be considered with caution, since there are several approximations regarding the lack of heat capacity dependence with temperature that have not been demonstrated for these systems. The observed negative values of ΔH° and ΔS° are in agreement with an enthalpy-driven process. From the comparison of these data with the previously reported for hevein and its structural analogs (Table 1) it is clear that the data indicates an enthalpy–entropy compensation phenomenon, a typical behavior for the association processes between lectins and neutral carbohydrates.[22]

There is a dramatic change in the association constant measured for the interaction between the Hev32S19D mutant with $(GlcNAc)_3$, compared with the original peptide Hev32. The Ser19 to Asp mutation probably eliminates an important intermolecular hydrogen bond with the carbonyl of one of the acetamide groups of chito-oligosaccharides in hevein and in truncated hevein,

Table 1
Association constants (K_a) at different temperatures (NMR and ITC) and thermodynamic parameters for hevein, Hev32, and Hev32S19D binding with $(GlcNAc)_3$ (*) and $(GlcNAc)_5$ (**)

	K_a [M^{-1}]				Thermodynamic parameters		
	T = 298 K	T = 303 K	T = 308 K	T = 313 K	ΔG [kJ mol^{-1}]	ΔH [kJ mol^{-1}]	ΔS [kJ mol^{-1}]
Hevein* (ITC)		8500			−22.6	−34.7	−41.4.
Hevein* (NMR)	11 500	8700	6900	5700	−23.0	−34.7	−44.7
Hevein** (ITC)	—	474,000	—	—	−32.6	−46.1	−45.0
Hev32* (NMR)	7700	4200	3400	2200	−21.8	−62.6	−136.0
Hev32S19D** (NMR)	2800	2400	2200	1400	−19.7	−33.7	−46.4
Hev32S19D* (NMR)	—	2400					
Hev32S19D*** (NMR)	150	110	90	80	−11.8	−26.2	−47.6

Ka of mutant peptide Hev32S19D binding (by NMR) with $(GlcNAc)_5$ (**) and $GlcNH_2\beta(1\text{-}4)(GlcNAc)_4$ (***). The affinity of Hev32S19D for $(GlcNAc)_3$ (*) and $(GlcNAc)_5$ (**). Estimated errors are smaller than 10%.

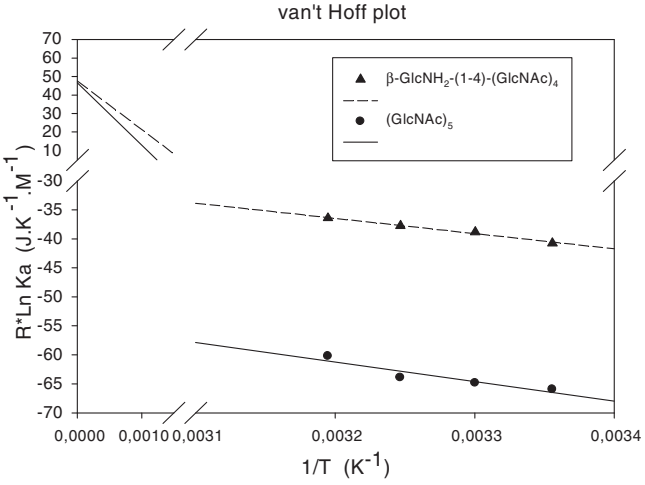

Figure 3. van't Hoff plots of ln K_a versus $1/T$ for both complexes.

Table 2
Structural statistics of the final ensemble of 20 CYANA conformers of the peptide free mutant Hev32S19D after refinement with AMBER 8

NMR restraints	
Distance restraints	
Total NOE crosspeaks assigned	1299
Total NOE upper distance limits	577
Short-range, $\|i-j\| \leqslant 1$	341
Medium-range, $1 < \|i-j\| < 5$	95
Long-range, $\|i-j\| \geqslant 5$	141
Restraint violations	
Maximum distance violation (Å)	7.57×10^{-2}
CYANA target function ($Å^2$)	7.04×10^{-2}
Structural statistics	
AMBER energy [kJ/mol(kcal/mol)]	-3.68×10^4 (-8.8×10^3)
RMSD from mean structure (Å)	
Backbone N, Cα, C′ of residues 3–31	0.53 ± 0.16
All heavy atoms of residues 3–31	1.19 ± 0.21
Ramachandran plot statistics (%)	
Residues in most favored regions (%)	58.5
Residues in additionally allowed regions (%)	41.5
Residues in generously allowed regions (%)	0
Residues in disallowed regions (%)	0

Hev32 (Scheme 2). Therefore, at a first glance, it may seem reasonable to conclude that the observed decrease in binding affinity is due to the loss of such hydrogen bond. Indeed, there is only a 2.1 kJ/mol difference in free energy between the truncated hevein and the S19D mutant. However, the $\Delta\Delta H^\circ$ amounts to ca. 29 kJ/mol, which seems too high for a single hydrogen bond (usually $\leqslant$ 10 kJ/mol). Nevertheless, at least part of the large entropic penalty associated with the recognition of the trisaccharide by Hev32 has been described in terms of a drastic rearrangement of the side chain of Trp21 between the free and $(GlcNAc)_3$-bound states, as evidenced by NOE and fluorescence data.[15,17] This change of orientation makes possible the existence of a proper match between the ligand and the lectin in terms of CH–π[23] and hydrogen bond interactions. In the mutant peptide, the lack of the key hydrogen bond mentioned above does not provide the driving force for the rearrangement of the Trp residue and thus, the entropy penalty is smaller. Nevertheless, the measured loss of 29 kJ/mol for the $\Delta\Delta H^\circ$ indicates that, in addition to the loss of the intermolecular hydrogen bond, no proper intermolecular stacking takes place, which could explain such a high loss in binding enthalpy. Indeed, no clear and strong intermolecular NOEs could be deduced for the mutant peptide–saccharide complex.

As no hydrogen bond can occur between the acetamide group and the Asp19 residue, we speculated that the newly introduced negative charge could be used to confer new specificity to the mutant hevein. We hypothesized that the aspartic carboxylate could engage in the formation of a salt bridge with a free amino group at the non-reducing end of a chitin analogue that would otherwise show low affinity for wild type hevein domains. To test our hypothesis, binding experiments were carried out with a chitosan derivative without the acetyl group at the non-reducing end of a chitopentasaccharide (Scheme 1). However, the measured affinity was even lower for the chitosan analogue than that measured for the chito-oligosaccharide. There is an additional loss in binding affinity for the chitosan derivative of 7.9 kJ/mol, from the enthalpy term. In principle, this additional loss of binding energy could be due to the complete loss of the CH–π interaction between the methyl acetamide group (which is absent in the chitosan derivative, Scheme 2) and Tyr30.

Thus, as a summary for these binding studies, the comparison of the data for the interaction of the mutant peptide Hev32S19D with the chito-oligosaccharide and with the chitosan analogue indicate that binding enthalpy is higher ($\Delta H^\circ = -33.7$ kJ/mol) when the acetyl group is present than when it is absent ($\Delta H^\circ = -26.2$ kJ mol^{-1}). This difference can be attributed to the absence of the acetamide group in the chitosan analogue and the consequent loss of a H-bond between its carbonyl and the Tyr OH as well as the stacking interaction between the methyl group and aromatic ring of the Tyr30. The observed entropic penalty is similar for the chito-oligosaccharide and for the $GlcNH_2(GlcNAc)_4$ chitosan analogue.

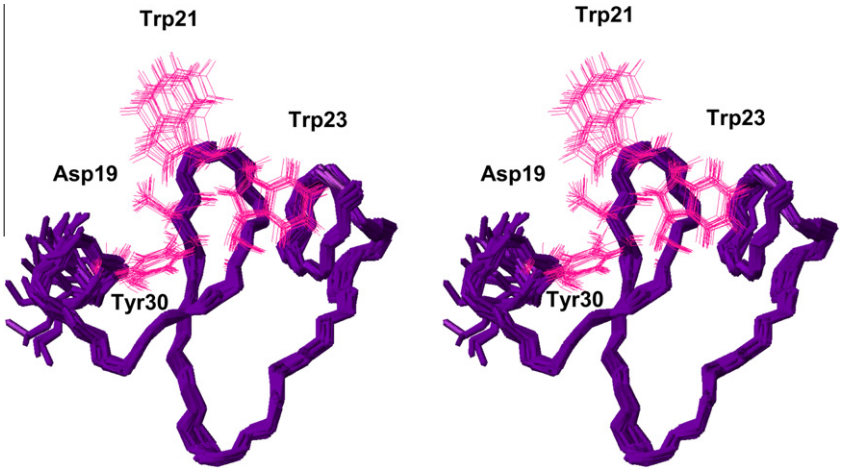

Figure 4. Stereoview of the superimposition of the backbone of 20 'best' NMR structures for the free peptide, Hev32S19D. The backbone atoms (2–29) were used for the superimposition.

2.2. The three-dimensional NMR structure of Hev32S19D

As a further step, in order to show the changes (if any) between the structure of the mutant peptide and its parent molecule, the solution NMR structure of HEV32S19D was deduced. The assignment of the ^{1}H NMR spectrum for the free mutant peptide HEV32S19D was determined using standard procedures based on 2D TOCSY and NOESY spectra recorded with different mixing times. The data were compared to those reported for the Hev32 analogue.[17]

The corresponding data are summarized in Table 2. A total of 1299 NOE cross peaks were identified, from which 577, unambiguously assigned by CYANA,[24] were employed as significant upper distance limits, divided into: short range (341), medium range (95), and long range (141). The best 20 CYANA conformers were then submitted to an energy refinement and optimization by using the AMBER force field,[25] including explicit water molecules. The good definition of the final structures is reflected in the average backbone RMSD value, which was 0.82 Å and 1.42 Å for all heavy atoms (Fig. 4). The goodness of the obtained structures was further corroborated by evaluation of the Ramachandran plot. Indeed, more than 95% of the φ/ψ torsion angle values are located in the most favored regions, as evaluated by the PROCHECK_NMR program. The orientation of the side chains is also fairly well defined (Fig. 4).

2.3. Structural comparison of the peptide Hev32S19D with Hev32

The comparative structural analysis of the peptide Hev32S19D with the structure of the parent Hev32, previously reported[17] showed that the geometry of the backbone is indeed very similar (Fig. 6). Moreover, there are no significant variations in orientation of the aromatic rings of the key amino acids, Trp23 and Tyr30 with respect to that in parent Hev32, which are crucial for oligosaccharide recognition, with some minor differences regarding Trp21. However, the presentation of the side chain of Asp19 (mutation point) differs of that of Ser19 in Hev32 (Fig. 6). In fact, this new orientation of the side chain of Asp makes possible the existence of a hydrogen bond between the carboxyl group and the HN of Gln20 (C═O···H–N distance smaller than 2.0 Å). These facts are, very probably, also at the origin of the low association constant obtained for the Hev32S19D–$(GlcNAc)_5$ complex. Because the carboxyl group of Asp19 is involved in this intramolecular hydrogen bond, no intermolecular hydrogen bond can take place between the sugar and the peptide and thus, the binding affinity is significantly decreased. Furthermore, the orientation of the Asp chain also precludes the establishment of a salt bridge type interaction with the free amine of the chitosan derivative that could partially restore binding. All these minor, but specific, geometrical considerations permit to explain the variations in affinity between the mutant and the parent Hev32 peptide and, thus, impose a free energy estimation of around 8–9 kJ/mol for the key hydroxyl–carbonyl (S19) hydrogen bond and for the stacking interaction between the GlcNAc acetamide methyl group and the aromatic ring of the Tyr30.

2.4. Conclusions

Our NMR studies of the interaction of the mutant peptide Hev32S19D with chitin fragments (and chitosan analogues) allowed us to estimate their affinity constants and associated thermodynamic data, which indicate that the mutant peptide is able to bind chitin oligomers. However, significant decreases in the association constants with chito-oligosaccharides are observed, when compared to those previously reported for hevein and truncated hevein (Hev32). The determination of the three-dimensional structure of the peptide mutant, by using two-dimensional NMR, has permitted us to deduce that the topology of the backbone is very similar to that of the parent Hev32 peptide. The same is true regarding the orientations of the key aromatic residues Trp23, and Tyr30, with some minor differences regarding Trp21. The decrease in the association constants can be attributed to the different topological orientation of the side chain of Asp19 of Hev32S19D, when compared to that of the 'natural' Ser19 of Hev32. Hence, the above-mentioned result clearly demonstrates the importance of the hydrogen bond between Ser19 OH and the acetamide carbonyl group of the carbohydrate, which crucially contributes to the stability and specificity of the molecular recognition process of chito-oligosaccharides by hevein domains.

On the other hand, the mutant peptide is not able to recognize in a significant way a chitosan analogue (N-deacetylated pentasaccharide at the non-reducing end), indicating that the presence of the acetamide moiety and the stacking interactions in which it can engage with the aromatic ring of Tyr30 are essential for the molecular recognition event. Furthermore, the hydrogen bond between the Ser19 hydroxyl group and the acetamide moiety of the sugar can not be mimicked by a salt bridge between D19 and the basic amine of the new glucosamine residue. The geometrical considerations permit to explain the variations in affinity between the mutant and the parent Hev32 peptide and, thus, impose a free energy esti-

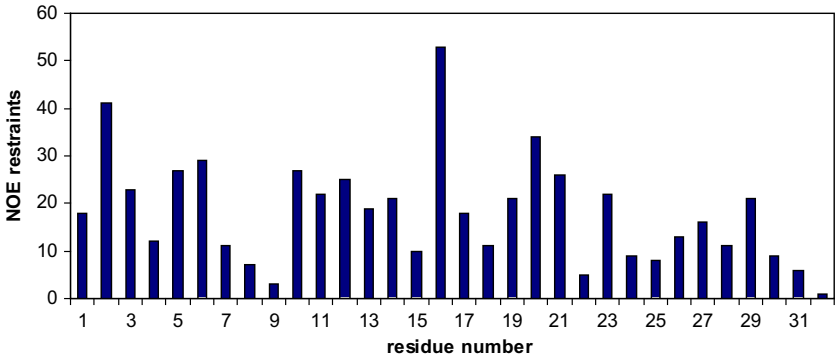

Figure 5. Number of NOE restraints for found for the different protons of the amino acid residues of the polypeptide chain.

mation of around 8–9 kJ/mol each for the key hydroxyl–carbonyl (S19) hydrogen bond, and for the stacking interaction between the GlcNAc acetamide methyl group and the aromatic ring of the Tyr30. The additional hydrogen bond interaction between the hydroxyl group of Tyr30 and one hydroxyl group of the sugar (with C3-OH), which can only be formed if the proper methyl-aromatic stacking mentioned above takes simultaneously place is also significant,[15,17,20,21] although smaller (ca. 2 kJ/mol). All these features seem to be essential to effectively recognize GlcNAc-containing saccharides. Very recently, exploiting these interactions, it has been possible to bind GlcNAc in a selective manner, by employing a designed synthetic receptor.[26] Further knowledge of the structural and energetic details of the interaction requirements for sugar binding may open new ideas and strategies for their effective recognition.

3. Experimental section

Oligosaccharides were purchased from Toronto Chemical Co. The chitosan analogous was a generous gift from Dr. E. Samain and Dr. H. Driguez (CERMAV, Grenoble).

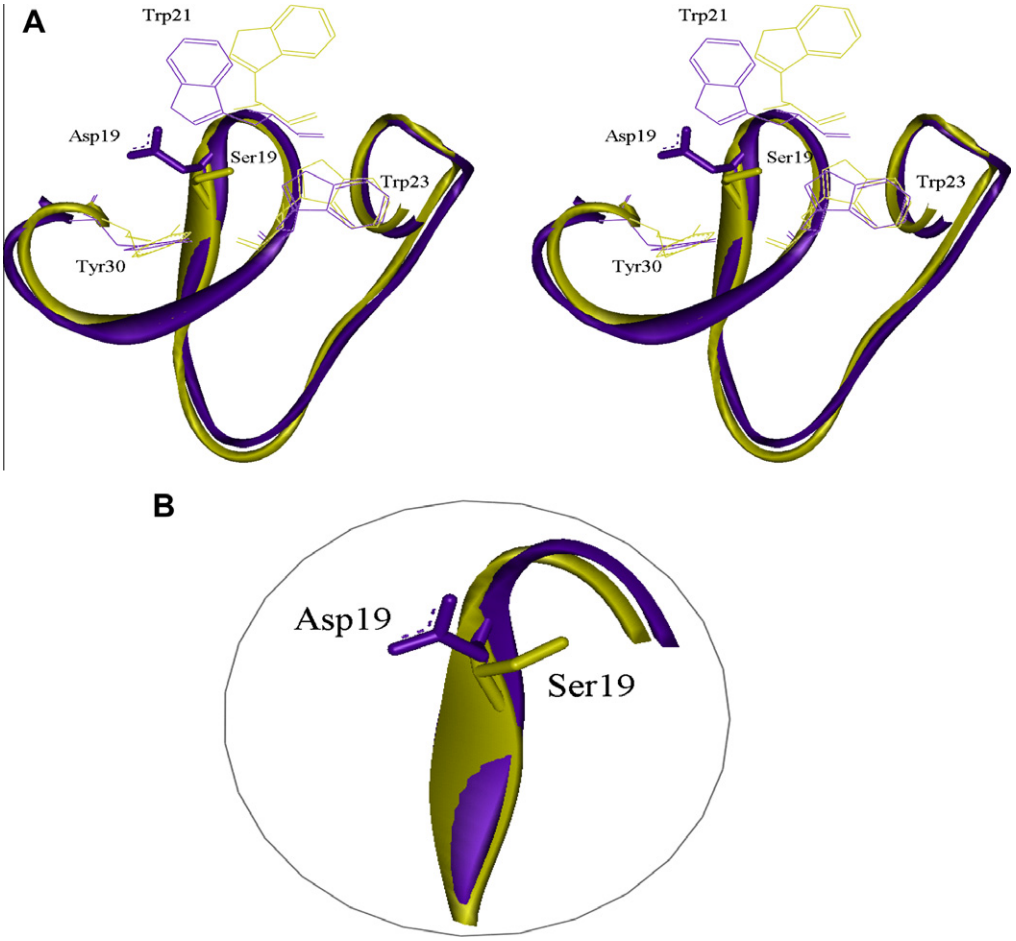

Figure 6. (a) Schematic ribbon stereoview representation of the backbone superimposition of the free mutant peptide Hev32S19D (dark violet) and Hev32 when bound to $(GlcNAc)_3$ (gold). The key amino acids at the binding site are highlighted. (b) Detailed view of the different orientation of the polar side chain of S19 in hevein and D19 in the corresponding mutant.

3.1. Peptide synthesis

Hev32S19D was synthesized as a C-terminal carboxamide on a Rink-amide MBHA resin using standard Fmoc solid phase peptide synthesis protocols. After chain assembly and cleavage from the resin the fully reduced peptide was purified by RP-HPLC to homogeneity. Oxidative folding of the hexathiol precursor was carried out at 25 μM peptide concentration under Ar atmosphere in 0.1 M Tris–HCl, 1 mM EDTA, pH 8.0 in the presence of reduced and oxidized glutathione (100:10 molar ratio relative to the peptide). Reaction was monitored by HPLC and MALDI-TOF MS and upon completion quenched by addition of TFA and purified by preparative RP-HPLC. The final product was further characterized by MALDI-TOF MS, amino acid analysis and NMR (see below). The typical chemical shifts for hevein domains were found thus assessing the proper disulfide formation for these peptides.

3.2. Titration experiments NMR spectroscopy

Titration experiments were performed by recording series of 1D ^{1}H NMR spectra, in a Bruker Avance 500 MHz spectrometer, for different mixtures of the mutant peptide Hev32S19D with $(GlcNAc)_5$ and with $GlcNH_2(GlcNAc)_4$, following the procedure previously described.[17]

Firstly, the spectra of ^{1}H NMR of two samples were recorded: for one 0.5 mL aliquot of a 5 mL solution of Hev32S19D, as zero point of the titration, and for a 0.5 mL aliquot of a 5 mL solution of a mixture of Hev32S19D (0.28 mM) and the corresponding carbohydrate (8 mM), as final point of the titration, corresponding to highest ligand–peptide ratio (ca. 29:1). To build up the titration curve, small aliquots of the highest ligand–peptide ratio to the ligand-free peptide sample were added in a systematic way, as previously described.[17] For each sample, with different concentrations of carbohydrate and the same concentration of mutant polypeptide, the ^{1}H NMR spectra were acquired at four different temperatures (298, 303, 308, 313 K). These data allowed to qualitatively estimate the thermodynamic parameters (ΔS and ΔH) of the interaction of the Hev32S91D polypeptide with both oligosaccharides, using van't Hoff plots. It should be recognized that the use of van't Hoff plots should be considered with caution, since there are several approximations regarding the lack of heat capacity dependence with temperature that have not been demonstrated for these systems.

3.3. 2D experiments for assignments and structure calculations

The corresponding spectra were recorded at 800 MHz in a Bruker Avance spectrometer. The samples for free and bound Hev32S19D (0.5 mM) were prepared in a buffer (90% H_2O–10% D_2O, 100 mM NaCl, 20 mM NaH_2PO_4, pH 5.6). TOCSY[27] (50 and 70 ms of mixing time) experiments were performed using standard sequences at 298 K, using the Watergate module for water suppression. NOESY[28] experiments were acquired with 200 and 300 ms of mixing times at 298 K, using the Watergate module for water suppression. The NMR data and coordinates are available from the authors.

3.4. Structure calculations

The three-dimensional structure of Hev32S129D was determined from the assigned NOESY cross peaks intensities (see Fig. 5 for the number of NOEs per residue). In a first step, the spin systems of all amino acids that constitute the polypeptide hev32S19D were assigned through the XEASY program.[29] Subsequently, the cross peaks volumes were determined by the automated peak integration routine, peakint, implemented in XEASY.[29] The CYANA program (version 2.1) was used to calculate the structure, following the standard protocol through seven iterative cycles, starting with 100 randomized conformers. The 20 best conformers, with the lowest final CYANA target function values, were retained for analysis and used as starting geometries for the next cycle. The final 20 CYANA structures were minimized in a box of explicit water molecules, using the conjugated gradient method, with the AMBER 9 program.[25] The free and complexed mutant peptides were immersed in a TIP3P water box (between 2649 and 3000 molecules, depending on the case), with a thickness of 10 Å. The restrained energy minimization process was carried out as follows: initially, in order to eliminate the bad contacts between the water molecules and the polypeptide, a 500-step minimization was performed only to the water molecules, keeping fixed the position of the peptide atoms, and using a force constant of 100 kcal/mol and constant volume. A subsequent minimization was then carried out where the peptide was relaxed with the NOE-based experimental restrictions and the water molecules were kept fixed. Finally, the restrained energy minimization was performed taking into account both the solvent and the peptide, using 3000 steps with the force field of Cornell et al.[30]

Acknowledgments

Financial support form MICINN-Spain is gratefully acknowledged (Grant CTQ2009-8536). We also thank UNAM (México) for a leave of absence for M. I. Chávez. We are grateful to Drs. H. Driguez and E. Samain (CERMAV-CNRS, Grenoble, France) for the chitosan derivative.

References

1. Solís, D.; Jiménez-Barbero, J.; Kaltner, H.; Romero, A.; Siebert, H. C.; von der Lieth, C. W.; Gabius, H. J. *Cells Tissues Organs* **2001**, *168*, 5–23.
2. *Protein–Carbohydrate Interactions and Infectious Diseases*; Bewley, C., Ed.; The Royal Society of Chemistry, 2005.
3. van Damme, E. J. M.; Peumans, W. J.; Pustazi, A.; Bardocz, S. *Handbook of Plant Lectins: Properties and Biomedical Applications*; Wiley-VCH, 1998.
4. Rodríguez-Romero, A.; Ravichandran, K. G.; Soriano-Garcia, M. *FEBS Lett.* **1991**, *291*, 307–309.
5. Wagner, S.; Breitneder, H. *Biochem. Soc. Trans.* **2002**, *30*, 935–940.
6. Dam, T. K.; Brewer, F. *Chem. Rev.* **2002**, *102*, 387–429.
7. Gabius, H.-J.; Siebert, H.-C.; André, S.; Jiménez-Barbero, J.; Rüdiger, H. *ChemBioChem* **2004**, *5*, 740–764.
8. Woods, R. J. *Glycoconjugate J.* **1998**, *15*, 209–216.
9. Jimenez-Barbero, J.; Asensio, J. L.; Cañada, F. J.; Poveda, A. *Curr. Opin. Struct. Biol.* **1999**, *9*, 549–555.
10. Imberty, A.; Perez, S. *Chem. Rev.* **2000**, *100*, 4567–4588.
11. Bewley, C. A. *Struct. Fol. Des.* **2001**, *9*, 931–940.
12. Wolmald, M. R.; Petrescu, A. J.; Pao, Y. L.; Gilthero, A.; Elliott, T.; Dwek, R. A. *Chem. Rev.* **2002**, *102*, 371–386.
13. Neuman, D.; Lehr, C.-M.; Lenhof, H.-P.; Kohlbacher, O. *Adv. Drug Delivery Rev.* **2004**, *56*, 437–457.
14. Puri, K. D.; Surolia, A. *Pure Appl. Chem.* **1994**, *66*, 497–502.
15. Chávez, M. I.; Andreu, C.; Vidal, P.; Aboitiz, N.; Freire, F.; Groves, P.; Asensio, J. L.; Asensio, G.; Muraki, M.; Cañada, F. J.; Jiménez-Barbero, J. *Chem. Eur. J.* **2005**, *11*, 7060–7074.
16. (a) Quiocho, F. A. *Pure Appl. Chem.* **1989**, *61*, 1293–1306; (b) Vyas, N. K. *Curr. Opin. Struct. Biol.* **1991**, *1*, 732–740.
17. Aboitiz, N.; Vila-Perelló, M.; Groves, P.; Asensio, J. L.; Andreu, D.; Cañada, F. J.; Jiménez-Barbero, J. *ChemBioChem* **2004**, *5*, 1–12.
18. Filion, D.; Lavertu, M.; Buschmann, M. D. *Biomacromolecules* **2007**, *8*, 3224–3234.
19. Shamov, M. V.; Bratskaya, S. Y.; Avramenko, V. A. *J. Colloid Interface Sci.* **2002**, *249*, 316–321.
20. (a) Asensio, J. L.; Siebert, H. C.; von Der Lieth, C. W.; Laynez, J.; Bruix, M.; Soedjanaamadja, U. M.; Beintema, J. J.; Canada, F. J.; Gabius, H. J.; Jimenez-Barbero, J. *Proteins* **2000**, *40*, 218–236; (b) Asensio, J. L.; Canada, F. J.; Siebert, H. C.; Laynez, J.; Poveda, A.; Nieto, P. M.; Soedjanaamadja, U. M.; Gabius, H. J.; Jimenez-Barbero, J. *Chem. Biol.* **2000**, *7*, 529–543; (c) Jimenez-Barbero, J.; Canada, F. J.; Asensio, J. L.; Aboitiz, N.; Vidal, P.; Canales, A.; Groves, P.; Gabius, H.-J.; Siebert, H.-C. *Adv. Carbohydr. Chem. Biochem.* **2006**, *60*, 303–354.
21. Asensio, J. L.; Canada, F. J.; Bruix, M.; Gonzalez, C.; Khiar, N.; Rodriguez-Romero, A.; Jimenez-Barbero, J. *Glycobiology* **1998**, *8*, 569–577.
22. Toone, E. J. *Curr. Opin. Struct. Biol.* **1994**, *4*, 719–728.
23. (a) Fernández-Alonso, M. C.; Cañada, F. J.; Jiménez-Barbero, J.; Cuevas, G. *J. Am. Chem. Soc.* **2005**, *127*, 7379–7386; (b) Vandenbussche, S.; Dolores Dıaz, D.; Fernandez-Alonso, M. C.; Pan, W.; Vincent, S. P.; Cuevas, G.; Cañada, F. J.; Jiménez-Barbero, J. *K., K. B. Chem. Eur. J.* **2008**, *14*, 7570–7578; (c) Terraneo, G.;

Potenza, D.; Canales, A.; Jiménez-Barbero, J.; Baldridge, K. K.; Bernardi, A. *J. Am. Chem. Soc.* **2007**, *129*, 2890–2900.
24. Güntert, P. *Methods Mol. Biol.* **2004**, *278*, 353–378.
25. Pearlman, D. A.; Case, D. A.; Caldewell, J. W.; Cheatham, T. E.; Debolt, S.; Ferguson, D.; Seibel, G.; Kollman, P. A. *Comput. Phys. Commun.* **1995**, *91*, 1–41.
26. Ferrand, Y.; Klein, E.; Barwell, N. P.; Crump, M. P.; Jiménez-Barbero, J.; Vicent, C.; Boons, G. J.; Ingale, S.; Davis, A. P. *Angew. Chem., Int. Ed.* **2009**, *48*, 1775–1779.
27. Bax, A.; Davis, D. G. *J. Magn. Reson.* **1985**, *65*, 355–360.
28. Kumar, A.; Ernst, R. R.; Wüthrich, K. *Biochem. Biophys. Res. Commun.* **1980**, *95*, 1–6.
29. Bartels, C.; Xia, T. H.; Güntert, P.; Wüthrich, K. J. *Biomol. NMR* **1995**, *6*, 1–10.
30. Cornell, W. D.; Cieplak, P.; Bayly, C. I.; Gould, I. R.; Merz, K. M.; Ferguson, D. M.; Spellmeyer, D. C.; Fox, T.; Caldewell, J. W.; Kollman, P. A. *J. Am. Chem. Soc.* **1995**, *117*, 5179–5197.